2021 EAGE ANNUAL
82ND CONFERENCE & EXHIBITION
AMSTERDAM | THE NETHERLANDS

A PRACTICAL IMPLEMENTATION OF CONVERTED-WAVE REFLECTION FULL-WAVEFORM INVERSION

N. Masmoudi[1], A. Ratcliffe[1], M. Wang[1], Y. Xie[1], T. Wang[2]

[1] CGG; [2] Tongji University

Summary

Depth imaging of converted-wave (P-to-S) ocean-bottom seismic (OBS) data requires a depth model for both the P- and S-wave velocities. Building the S-wave velocity model is very challenging: conventional techniques include PP and PS image registration, or joint PP and PS tomography. These approaches are often impeded by the lack of a reliable PS image in the shallow part of the model due to the sparse-receiver acquisition of typical OBS surveys, and have limited resolution to deal with complex lateral velocity variations. We introduce a new full-waveform inversion technique to update the S-wave velocity using converted-wave reflection data recorded in the radial component of OBS surveys. Key aspects of the method include the use of acoustic Born-modeling, a robust objective function to handle kinematic and dynamic differences, and a layer-stripping strategy to simplify the non-linearity of the inversion problem. The proposed approach is validated on different synthetics, and demonstrated on a field data example, giving an improved S-wave velocity and better reflector continuity for PS imaging.

A practical implementation of converted-wave reflection full-waveform inversion

Introduction

Ocean-bottom seismic (OBS) surveys record and utilize compressional (P) and shear (S) wave modes. This allows the imaging of converted-wave, or PS, data generated from a down-going P-wave converting into an up-going S-wave at the reflection point. As P and S waves provide complementary elastic parameter information, converted waves are useful for characterizing properties of reservoirs. For example, comparison of PP and PS images can help identify fluid contacts and S-wave ray paths provide a tool to illuminate targets hidden beneath gas-filled zones.

Depth imaging of the radial component of converted-wave PS data requires a consistent depth model for both P and S velocities. Full-waveform inversion (FWI) is an important tool for building accurate P-wave velocity (V_P) models, especially for complex overburdens. Since multi-parameter elastic-FWI updating S-wave velocity (V_S) is not yet adopted in the industry due to its cost and complexity, there is still a lack of an equivalent FWI tool for V_S model building. Techniques such as PP and PS image registration, or joint PP and PS tomography, are typically used instead. However, PS registration is often impeded by the lack of a reliable PS image in the shallow part of the model due to the sparse acquisition of typical OBS surveys, and tomography has limited resolution to deal with complex lateral velocity variations. Clearly, V_S model building for converted-wave imaging remains an ongoing challenge.

We propose an FWI approach to update the V_S model using converted-wave PS-reflection events recorded in the radial component of OBS data (PS-RFWI). Our approach uses Born-modeling to explicitly compute the low-wavenumber kernels along the different up- and down-going source-and-receiver side wavefields, similar to the PP reflection-FWI strategies developed in Xu et al. (2012) and Brossier et al. (2014). It is well-known from these, and other works, that reflection-FWI is a very difficult problem. Hence, to make the PS version more tractable, we assume prior knowledge of the V_P model and PP reflectivity (e.g. obtained from FWI of pressure data), and we focus our PS-RFWI to invert only for V_S, although a joint V_P and V_S scheme is possible. These assumptions avoid the reflectivity update at each FWI iteration, as well as mitigating crosstalk between V_P and V_S. Further, we use acoustic Born-modeling to reproduce the PS kinematics, and handle the resulting observed/modeled amplitude differences, as well as the potential cycle skipping issues due to an inaccurate starting V_S model, with a robust objective function based on partial matching (Cooper et al., 2020).

PS Born-modeling

PS-reflection modeled data are obtained from a demigration process, which can be expressed for the simple acoustic, constant density, wave equation case, as follows:

$$\frac{1}{V_{0_P}^2}\frac{\partial^2 p}{\partial t^2} - \nabla^2 p = f, \tag{1}$$

$$\frac{1}{V_{0_S}^2}\frac{\partial^2 \delta p}{\partial t^2} - \nabla^2 \delta p = \delta f(p, V_{0_P}, I), \tag{2}$$

where p is the incident P-wavefield propagating in the background V_{0_P} model, δp is the scattered (demigrated) S-wavefield propagating in the background V_{0_S} model, f is the source wavelet, δf is the source for the demigration step, and I is the reflectivity image. When modeling data using reciprocity (as it is often the case for OBS surveys), we need to swap V_{0_P} and V_{0_S} in Equations (1) and (2). This acoustic demigration process reproduces the kinematics of recorded PS data, although the amplitude behavior relative to the observed data is different, similar to any acoustically modeled data.

PS-RFWI gradient

The goal of PS-RFWI is to minimize the difference between the observed and modeled PS data through optimization of an objective function, J. In the scheme proposed here J should preferably mitigate amplitude errors due to the acoustic modeling as well. Let $\boldsymbol{m_0}$ be the vector containing the background medium parameters $V_{0_P}$and V_{0_S}, and $F(\boldsymbol{m_0})$ and $\delta F(\boldsymbol{m_0}, I)$ be the recorded data obtained from Equations (1) and (2), respectively. The gradient of PS-RFWI with respect to one of the model parameter m_0^i can be efficiently obtained via the adjoint-state method, as follows:

$$\frac{\partial J}{\partial m_0^i} = \int_{t=0}^{tmax} \frac{\partial F(\boldsymbol{m_0}, t)}{\partial m_0^i}\, \delta R(\boldsymbol{m_0}, I, t) + \frac{\partial \delta F(\boldsymbol{m_0}, I, t)}{\partial m_0^i}\, R(\boldsymbol{m_0}, I, t)\, dt, \quad (3)$$

where δR is the scattered adjoint wavefield, obtained by demigration of the adjoint wavefield R. The first term in the gradient expression is the correlation of a down-going source-side wavefield with an up-going receiver-side reflected wavefield, and the second term is the correlation of an up-going source-side reflected wavefield with a down-going receiver-side wavefield – together these generate the so-called 'rabbit ears' in reflection FWI (see Figure 1a). For PS data, the first term in Equation (3) contributes to the V_{0_P} gradient, and only the second term contributes to the V_{0_S} gradient (see Figure 1b). A joint-update of both V_{0_P} and V_{0_S} is very challenging due to the crosstalk between the two parameters, as well as the requirement of migrating PS data at every FWI iteration. Practically, it is simpler to derive a good V_{0_P} model and PP image using the pressure component, which subsequently can be kept fixed during PS-RFWI. This assumption allows PS-RFWI to focus only on the V_{0_S} update, hence mitigating the crosstalk problem and maintaining an efficient workflow. Finally, the choice of the PP image, instead of the PS image, for the reflectvity model is a practical measure justified by the potentially poor quality PS image in the shallow part of model (due to the sparse OBS acquisitions).

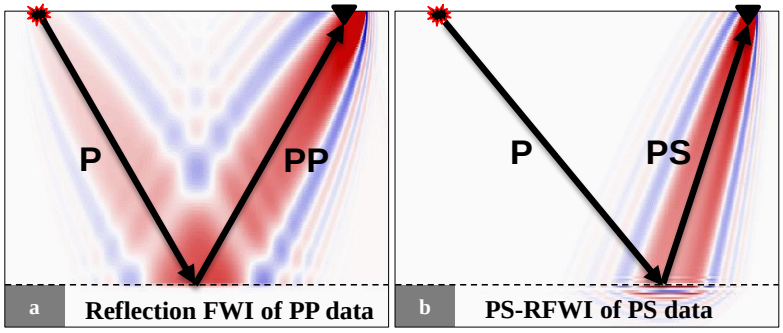

Figure 1 *Update kernels for a single-source, single-receiver geometry: (a) V_{0_P} kernel from reflection FWI of PP data, and (b) V_{0_S} kernel from PS-RFWI of PS data.*

Synthetic examples

Our first synthetic example is based on a simple 2D, equally spaced, layer-cake model, and a realistic ocean bottom node (OBN) geometry. Figure 2a shows the true V_S model ($V_P = 3V_S$) used to generate the radial component data. This is a non-inverse crime test where we use elastic forward modeling to generate the observed data and process this data to keep PS events only. The starting V_S model (Figure 2b) is a linearly increasing model with depth. Figures 2c and 2d show the PS-RFWI inverted model using the least-squares objective function without and with partial matching, respectively. Partial matching (Cooper et al., 2020) is a technique for mitigating cycle skipping in FWI. The method also accommodates some amplitude differences between observed and modeled data. The vertical V_S profiles in Figures 2e and 2f clearly show the benefit of including partial matching in the FWI.

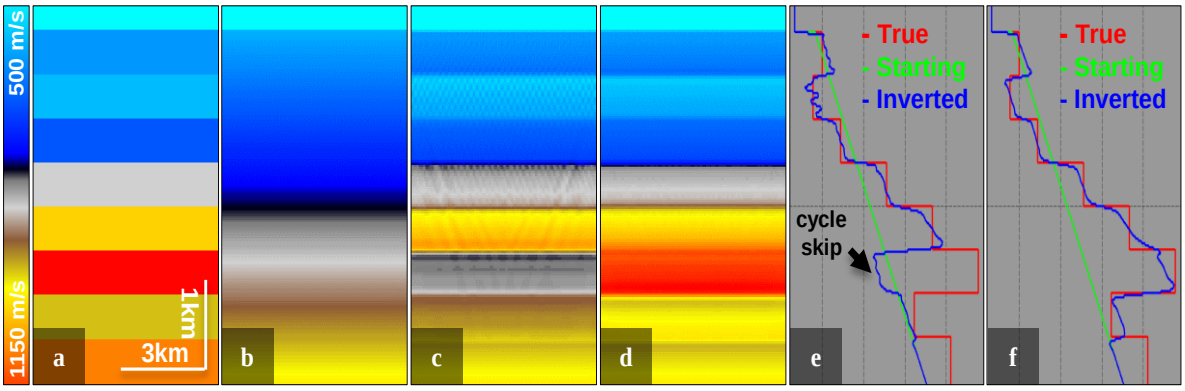

Figure 2 *Synthetic example based on a 1D layered model: (a) true V_S, (b) starting V_S, (c) inverted V_S without partial matching, and (d) inverted V_S with partial matching. Vertical V_S profiles: (e) without partial matching, and (f) with partial matching.*

Our second synthetic example is based on the more complex Chevron/SEG 2014 2D FWI model: we use a pre-existing V_P tomography model shown in Figure 3a (the true model has yet to be released by Chevron/SEG), create a V_S model such that $V_P/V_S=3$, and design a realistic OBN acquisition with 50 m and 200 m shot and receiver-node spacing, respectively. Figure 3c shows an example of elastically modeled, radial component data to 20 Hz, processed to remove PP events, while Figure 3b shows the equivalent, acoustically modeled, PS Born data. While the two modeling schemes have different amplitude behavior, we still generate kinematically accurate PS Born data even for this complex model.

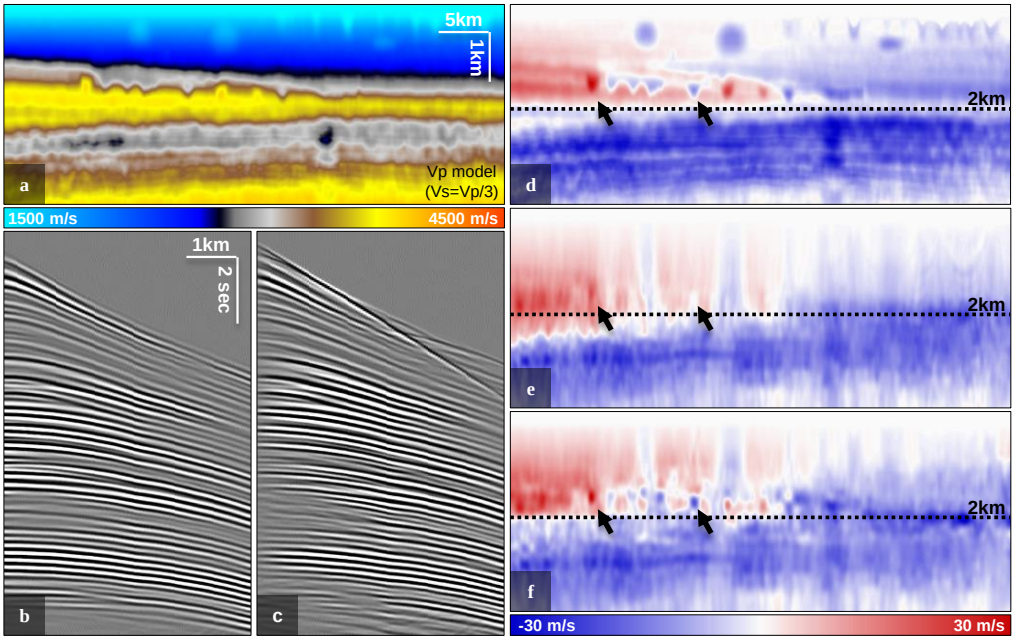

Figure 3 *Synthetic based on Chevron/SEG 2014 model: (a) V_P tomography model, (b) acoustic PS Born data, and (c) elastic forward modeled data. Inversion results: (d) true V_S perturbation, (e) V_S perturbation without layer stripping, and (f) V_S perturbation with layer stripping.*

For this second non-inverse crime synthetic, we create a V_S perturbation (Figure 3d) with similar features to the 'true' model. PS-RFWI is conducted for multiple frequency bands from 3 Hz to 10 Hz, where we use our pre-existing V_P and reflectivity models (that remain fixed during the inversion). Figure 3e shows our V_S perturbation after PS-RFWI. In general, the long-wavelength components of the true perturbation are recovered. Moreover, as expected from an FWI that is reliant on reflection data only, the vertical resolution is typically worse than the lateral resolution, this resolution being driven by the presence (or absence) of reflectors (the so-called 'fingering effect' in reflection-FWI). This inversion can be improved by using a layer stripping strategy: we update the model from top to bottom, whereby we input the early arrivals to the inversion first, and include the later reflections progressively as we go deeper in the model update. This strategy results in the V_S perturbation shown in Figure 3f, which shows better recovery of the shallower anomalies, as well as a slightly reduced 'fingering effect' (see arrows).

Field data example

The field data example consists of a 4C OBN data set. First, converted-wave PS-events are extracted from the horizontal components via a radial direction rotation. Then, deconvolution of the radial and downgoing data (obtained from processing of the pressure and vertical components) allows, among other things, to remove free-surface related multiples (Wang et al., 2010). The pre-existing V_P velocity and PP reflectivity are high enough quality and are not updated in our PS-RFWI workflow. On the other hand, the extremely low V_S in the shallow layer sediments (~50 m/s), as well as the sparse node acquisition (300 m node spacing), pose difficult challenges in this data. We opt for a two-stage, layer-stripping strategy, whereby we update the near surface first, then move down to the deeper section. Given the very low V_S, we limit the maximum inverted frequency to 4 Hz. We show here the results from the second stage update. Figure 4 compares the starting V_S and the corresponding migrated PS data to the final V_S and migrated PS data after PS-RFWI. The inverted V_S shows better consistency with the model structures (e.g. see red arrows). It also fixes many pull-up and push-down distortions, and results in better-migrated reflector continuity, as highlighted by the dashed boxes.

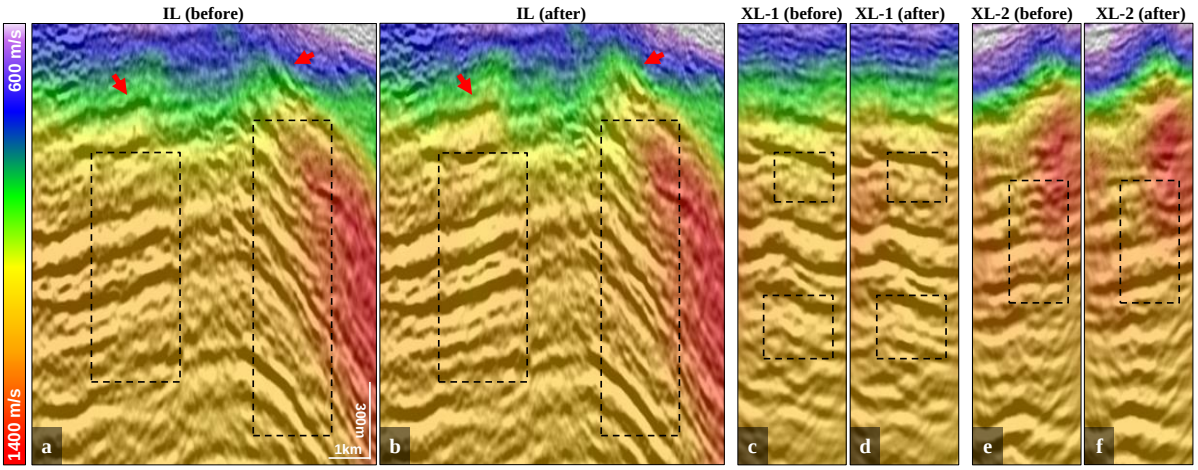

Figure 4 *V_S model overlaid on the migrated PS data for an inline (IL) and two crossline (XL) sections, respectively: (a), (c) and (e), before PS-RFWI; and (b), (d) and (f), after PS-RFWI.*

Discussion

Building a V_S model is a very challenging problem and our new approach adds another tool to the toolbox. We propose to rely on prior knowledge of the V_P model and PP reflectivity to alleviate some of the non-linearities of the problem; while a joint approach updating both V_P and V_S may be possible in the future, it is a non-trivial extension. In addition, we rely on the acoustic wave equation to generate our modeled PS data; elastic Born-modeling is another option but has cost and complexity implications. Further, extremely low V_S velocity values have a dramatic impact on the computational cost, while the often very uncertain starting model can cause extreme cycle skipping. Another factor in any PS work is the data processing required to isolate the PS events, which can be challenging for field data. Finally, while elastic FWI using diving waves, reflections and multiples should result in better model illumination and resolution, it comes at considerable extra cost and complexity.

Conclusions

We proposed a new FWI approach for updating the V_S model using PS converted-wave reflection data: acoustic Born-modeling, a robust objective function, and a prior knowledge of the PP reflectivity and V_P model are key aspects for the method's effectiveness. We validated the method on different synthetics and, for a complex field data example, demonstrated an improvement in the V_S model and a subsequent uplift in the migrated PS image.

Acknowledgements

We thank CGG for permission to publish this paper and TOTAL for permission to show the field data example. We also thank Ololade Bukola, Ramez Refaat, Jamie Richardson and Julian Holden for their assistance with the field data processing and velocity model building. We gratefully acknowledge Adriano Gomes for his initial work on PS-RFWI, James Cooper for his assistance with the partial matching approach, and Chevron/SEG for the FWI inspired synthetic.

References

Xu, S., Chen, F., Lambaré, G., Zhang, Y. and Wang. D. [2012] Inversion on reflected seismic wave. *82nd Annual International Meeting, SEG,* Expanded Abstracts, 1-7.

Brossier, R., Operto, S. and Virieux, J. [2014] Velocity model building from seismic reflection data by full-waveform inversion. *Geophysical Prospecting*, **63**, 354-367.

Cooper, J., Ratcliffe, A. and Poole. G. [2020] Mitigating cycle skipping in full-waveform inversion using partial matching filters. *82nd EAGE Conference and Exhibition,* Extended Abstracts, 1-5.

Wang, Y., Bale, R., Grion, S., and Holden, J. [2010] The ups and downs of ocean-bottom seismic processing: Applications of wavefield separationand up-down deconvolution. *The Leading Edge*, 29 (10), 1258-1265.